2

Topological entropy of one-dimensional deformed maps

2.1 INTRODUCTION

In this chapter, we apply type-1 and type-2 deformation schemes on the logistic map, and type-1 deformation on the Gaussian map to analyze the dynamics of these newly deformed maps. In Section 2.2, we analyze the q-logistic map of type-1 by calculating the basic dynamics like fixed points, periodic orbits and transition from periodicity to chaos. We calculate the topological entropy to show the existence of Li-Yorke chaos of the deformed logistic map. Further, we show that there exist a region of physically observable chaos, which is separated by the region where the chaos is not physically observable. In Section 2.3, we apply type-2 deformation on the logistic map, and discuss the similar analysis for the deformed logistic map. Finally in Section 2.4, we analyze the deformed Gaussian map with type-1 deformation and compute the topological entropy using the *Lap Number Method* to discuss the chaotic behaviour of the map.

We recall some basic definitions :

An interval map $f : [a,b] \to [a,b]$ is said to be *unimodal* if there exists a unique point $c \in (a,b)$, the *critical point*, where $Df(c) = 0$, such that f is strictly increasing in $[a,c)$ and strictly decreasing in $(c,b]$.

A critical point c of a map f is said to be *non-flat critical point* if there exists $n \in \mathbb{N}$ such that $D^n f(c) \neq 0$ and $D^k f(c) = 0$, where $1 \leq k < n$.
Here $D^n f$ denotes the n^{th} derivative of f.

Let f be a C^3 map. Then the *Schwarzian Derivative* f is denoted by $S(f)$, defined as

$$Sf(x) = \frac{D^3 f(x)}{Df(x)} - \frac{3}{2}\left(\frac{D^2 f(x)}{Df(x)}\right)^2.$$

A unimodal map f is called *S-unimodal* if it has negative Schwarzian derivative.

Let $I = [a,b]$ be a closed interval and let $f, g : I \to I$ be two maps. If there exist a homeomorphism $h : I \to I$ such that $h \circ f = g \circ h$ then f and g are said to be topologically conjugate. The homeomorphism h is called topological conjugacy.

2.2 Q-LOGISTIC MAP OF TYPE-1

One-dimensional logistic map is given by

$$f_a(x) = ax(1-x), \tag{2.1}$$

where the parameter $a \in [0,4]$ and $x \in [0,1]$.
Deformation of type-1 on real number x and deformation parameter q_1 is given by:

$$[x]_{q_1} = \frac{1-q_1^x}{1-q_1}, \tag{2.2}$$

where $q_1 \in \mathbb{R}$. As $q_1 \to 1$ the deformed number $[x]_{q_1} \to x$.
Consider this deformation $[x]_{q_1}$ on x of $f_a(x)$ then we obtain the following deformed logistic map:

$$\begin{aligned} f_a([x]_{q_1})(x) &= \frac{a(1-q_1^x)(q_1^x-q_1)}{(1-q_1)^2}, \\ &\equiv \mathscr{F}a,q_1(x), \end{aligned} \tag{2.3}$$

where $a \in [0,4]$, $x \in [0,1]$ and $q_1 \in (0,\infty)\backslash\{1\}$. As the limit $q_1 \to 1$, the deformed logistic map (2.3) approaches to the usual logistic map $f_a(x)$. We consider $q_1 \in (0,15) \setminus \{1\}$ in our discussion. This map is an interval map from $[0,1]$ to $[0,1]$ which attains the maximum value at critical point $C = \frac{\log((q_1+1)/2)}{\log(q_1)}$.

Let us consider $\mathscr{G}_{a,q_1}(x) = [\cdot]_{q_1} \circ f_a(x) = [f_a(x)]_{q_1}$ and the corresponding composition function is given by

$$\mathscr{G}_{a,q_1}(x) = \frac{1-q_1^{ax(1-x)}}{1-q_1}. \tag{2.4}$$

We call it as q-logistic map of type-1. The map $\mathscr{G}_{a,q_1}(x)$ is an interval map from [0,1] to [0,1] and has unique critical point at $x = 0.5$ for all $q_1 \in (0,\infty)\backslash\{1\}$ and $a \in [0,4]$.

Clearly, if two maps are topological conjugate to each other then it implies that they have similar dynamics. Since the map $\mathscr{G}_{a,q_1}(x)$ is topological conjugate to $\mathscr{F}_{a,q_1}(x)$, through the homeomorphism $[x]_{q_1}$. Then we have

$$\mathscr{G}_{a,q_1}(x) \circ [x]_{q_1} = [x]_{q_1} \circ \mathscr{F}_{a,q_1}(x).$$

As the dynamics of $\mathscr{F}_{a,q_1}(x)$ and $\mathscr{G}_{a,q_1}(x)$ are similar, it is more suitable to work with $\mathscr{G}_{a,q_1}(x)$ instead of $\mathscr{F}_{a,q_1}(x)$. Since $\mathscr{G}_{a,q_1}(x)$ has unique critical point whereas the map $\mathscr{F}_{a,q_1}(x)$ has different critical points depends on the value of q_1. Note that the critical point plays an important role in the study of kneading theory and other dynamics like finding Misiurewicz parameter.

Lemma 2.2.1. *The map $\mathscr{G}_{a,q_1} : I \to I$ is S-unimodal map and so $\mathscr{F}_{a,q_1}(x)$.*

Proof. Clearly, $\mathscr{G}_{a,q_1}(x)$ is C^∞-map with $\mathscr{G}_{a,q_1}(0) = \mathscr{G}_{a,q_1}(1) = 0$.

Further, $\mathscr{G}_{a,q_1}(x)$ has unique critical point at $x = 0.5$ for any value of a and q_1. Therefore,

$$\begin{aligned} S(\mathscr{G}_{a,q_1})(x) = S([\cdot]_{q_1} \circ f_a)(x) &= (S([\cdot]_{q_1}) \circ f_a(x)) \cdot (f_a'(x))^2 + S(f_a)(x), \\ &= -\frac{1}{2}(\log q_1)^2 \cdot (a(1-2x))^2 - \frac{6}{(1-2[x]_{q_1})^2}. \end{aligned}$$

This implies that $S(\mathscr{G}_{a,q_1})(x) < 0$ for all x. Hence $S(\mathscr{G}_{a,q_1})(x)$ is S-unimodal. Since $\mathscr{G}_{a,q_1}(x)$ is topological conjugate to $\mathscr{F}_{a,q_1}(x)$, so $\mathscr{F}_{a,q_1}(x)$ is also S-unimodal map. □

2.2.1 Fixed points and other attractors

We fix the parameter a and vary the deformed parameter q_1, then we notice that the map $\mathscr{G}_{a,q_1}(x)$ has three fixed points $\{0, x^*_+, x^*_-\}$ such that $0 < x^*_- < x^*_+$, the existence of these fixed points depends on the value of a and q_1. The fixed point $x^* = 0$ exists for all values of a and q_1. Further, it is stable for $a < (q_1 - 1)/(log(q_1))$. The fixed point x^*_+ undergoes reverse periodic doubling bifurcation route to chaos. The attractors lie on the period doubling route of x^*_+ coexists with $x^* = 0$ for the higher value of q_1. We notice that whenever two attractors coexists, the fixed point x^*_- exists as repeller between these attractors.

For a given value of parameter 'a', the fixed points of $\mathscr{G}_{a,q_1}(x)$ are shown in Fig. 2.1 as the deformed parameter q_1 varies. The black line represents the stable fixed point and grey line represents the unstable fixed point. In Fig. 2.1(i), the x^*_+ starts as stable fixed point (black colour) and bifurcates into period-2 orbit (where fixed point x^*_+ plotted in grey colour). The two black lines together shows coexistence of two stable fixed points and x^*_- is unstable fixed point between them. In the Fig. 2.1(ii), the fixed point x^*_+ is stable for higher value of q_1 beyond 15. The black line of $x^* = 0$ and unstable fixed point x^*_- shows that there are attractors en route of x^*_+ coexists with $x^* = 0$.

The size of the basin of fixed point x^* is the fraction of initial conditions attracted to the fixed point x^*, and it is denoted by $\omega(x^*)$. The size of the basin of the map $\mathscr{G}_{a,q_1}(x)$ for different a and q_1 values is shown in the Fig. 2.2(i). There are three conditions arise based on the value of $\omega(x^*)$ which are as follows:

1. $\omega(x^*) = 1$, the fixed point x^* is the unique attractor.

2. $\omega(x^*) = 0$, there is unique attractor which is either x^*_+ or other attractors (periodic attractor, a Cantor set or a transitive interval attractor) generates when x^*_+ become unstable.

3. $0 < \omega(x^*) < 1$, there are multiple attractors. As x^*_+ undergoes periodic doubling route to chaos, these attractors exists with the stable fixed point $x^* = 0$.

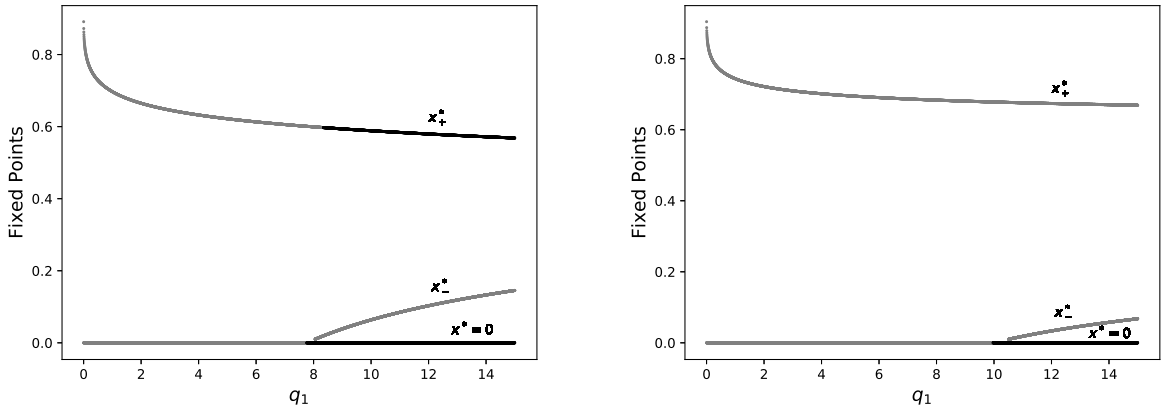

(i) $a = 3.3$ (ii) $a = 3.9$

Figure 2.1. : Fixed points of q-logistic map of type-1 $\mathscr{G}_{a,q_1}(x)$ for deformed parameter $q_1 \in (0.00001, 15)$.

The region R_1 represents $\omega(x^*) = 1$ that implies $x^* = 0$ is the only stable attractor. In the

region R_2, the size of the basin of $x^* = 0$ is 1 which are in general implies that all the trajectories in this region are converging to $x^* = 0$ but there are a set of disconnected points which are not converging to $x^* = 0$. This fact leads to the Proposition 2.2.2. The region R_3 indicates the area when $\omega(x^*) = 0$ that implies there is a unique metric attractor, which is different from $x^* = 0$. The region R_4 shows the coexistence of attractor (periodic or chaotic) where $0 < \omega(x^*) < 1$. Fig. 2.2(ii) shows the presence of stable fixed point x^* with the chaotic attractor based on positive Lyapunov exponent. We consider the initial condition $x_0 = 0.5$ for computing the Lyapunov exponent.

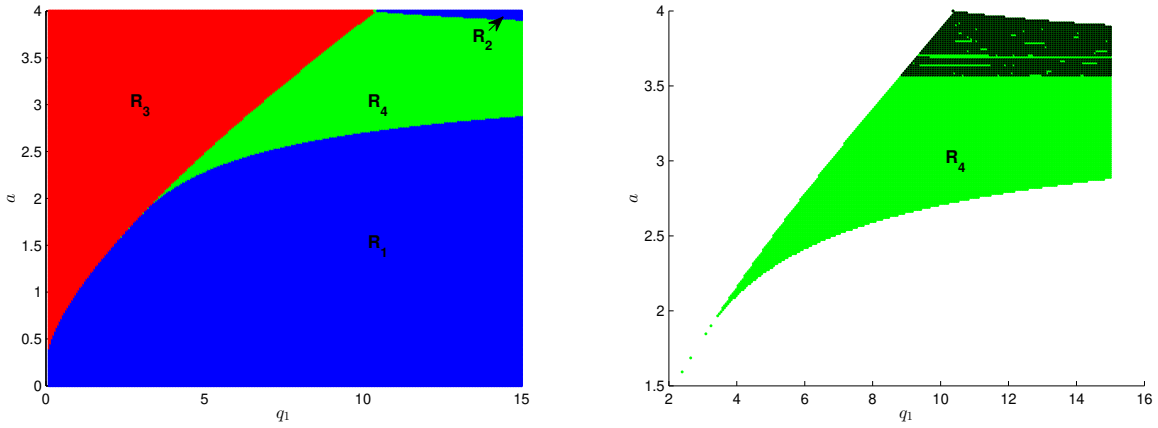

(i) (ii)

Figure 2.2. : (i) Basin of attraction of the fixed point $x^* = 0$, where the region $R_1 \cup R_2$ represents $\omega(x^*) = 1$, R_3 is for $\omega(x^*) = 0$ and R_4 is for $0 < \omega(x^*) < 1$; (ii) The region R_4 represents coexistence of attractors in which black colour shows the chaotic attractor based on positive Lyapunov exponent.

Proposition 2.2.2. *There is an open interval $(\gamma_1, \gamma_2) \subset [0,4]$ for every $(q_1, a) \in R_2$ such that there exists some states $x_i, x_j \in [0,1]$ for which there exists $n_0 \in \mathbb{N}$ such that*

$$\mathscr{G}^n_{a,q_1}(x_i) \to x^*_- \text{ and } \mathscr{G}^n_{a,q_1}(x_j) \to 0 \text{ for all } n \geq n_0.$$

Proof. We divide the interval $I = [0,1]$ into $J_1 = [0, x^*_-)$, $J_0 = [x^*_-, \alpha_1]$, $J_2 = (\alpha_1, 1]$, where $\alpha_1 = \mathscr{G}^{-1}_{a,q_1}(x^*_-)$.

All these intervals are shown in Fig. 2.3. To make notation simple, we use $\mathscr{G}(x)$ in place of $\mathscr{G}_{a,q_1}(x)$.

Suppose,

$$L_0 = \{x : \mathscr{G}(x) \in J_2 \text{ and } \mathscr{G}^2(x) \in J_1\}.$$

Clearly L_0 is an open interval containing the critical point c and L_0 leave J_0 in the first iteration. Further orbits of L_0 converges to $x^* = 0$.

Therefore $J_0 \backslash L_0$ have two closed intervals I_0 and I_1. Let

$$L_1 = \{x : \mathscr{G}(x) \in L_0\}.$$

If $x \in L_1$, then we have $\mathscr{G}(x) \in L_0$, $\mathscr{G}^2(x) \in J_2$, $\mathscr{G}^3(x) \in J_1$ and $\mathscr{G}^n(x) \to 0$.

Further L_1 contains two open intervals $L_{1,1}$ in I_0 and $L_{1,2}$ in I_1, which leave J_0 in second iteration and falls into J_1 in the third iteration. The future orbits of L_1 converges to $x^* = 0$.

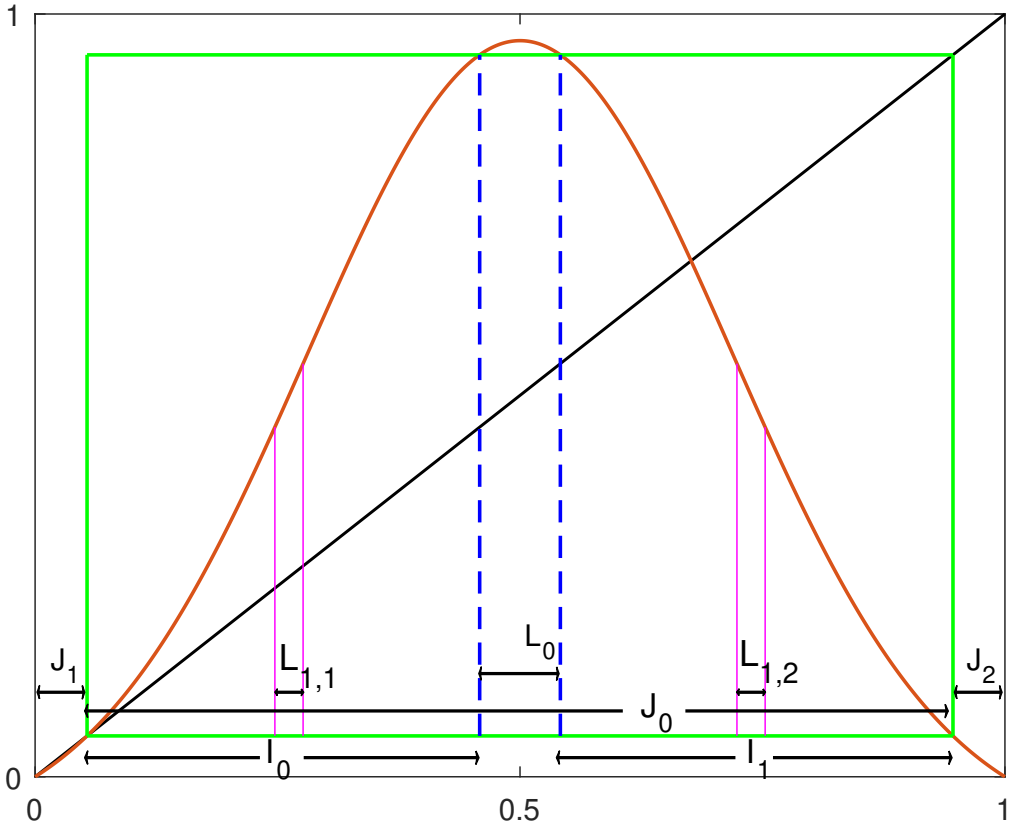

Figure 2.3. : The q-logistic map of type-1 $\mathscr{G}_{a,q_1}(x)$ at $q_1 = 14$ and $a = 3.95$.

Clearly, $J_0 \backslash \{L_0 \cup L_1\}$ contains four closed intervals which maps onto I_0 and I_1 by $\mathscr{G}$. In the second iteration of $\mathscr{G}$, these intervals maps onto J_0. The L_2 contains four open subintervals $L_{2,k}$ for $1 \leq k \leq 4$ in these closed intervals. The $L_{2,k}$ mapped onto L_0 by $\mathscr{G}^2$ and points of $L_{2,k}$ leave J_0 in the third iteration of $\mathscr{G}$. The interval

$$L_2 = \{x : \mathscr{G}^2(x) \in L_0\}.$$

Continuing in the similar manner, the construction of L_n is

$$L_n = \{x : \mathscr{G}^n(x) \in L_0\},$$

which is similar as

$$L_n = \{x \in J_0 : \mathscr{G}^i(x) \in J_0 \text{ for } 0 \leq i \leq n, \text{ but } \mathscr{G}^{n+1}(x) \in J_2 \text{ and } \mathscr{G}^{n+2}(x) \in J_1\}$$

The L_n contains 2^n open intervals $L_{n,k}$ where $1 \leq k \leq 2^n$. Points of $L_{n,k}$ leave J_0 in $(n+1)^{\text{th}}$ iteration and ultimately converges to $x^* = 0$.

The set of points $x_i \in \Gamma = J_0 \backslash \left(\bigcup_{n=0}^{\infty} L_n \right)$ will never escape J_0. The rest of the points $x_j \in I - \Gamma$ converges to the fixed point $x^* = 0$. □

From the above proposition, we conclude that there exists a Cantor set Γ which is invariant under the map $\mathscr{G}_{a,q_1}(x)$ and therefore the orbits of points in this set do not converge to zero.

2.2.2 Topological entropy

Topological entropy was introduced by Adler et al. on compact metric space $\mathbb{X}$ [Adler *et al.*, 1965]. The topological entropy of any open cover u of compact space $\mathbb{X}$ as $H(u) = \log N(u)$, where $N(u)$ denotes the number of sets in a subcover of minimal cardinality.

Topological Entropy: Assume that f is piecewise strictly monotone mapping of an interval. Let c_n be the number of points at which f^n has extrema. Then according to [Misiurewicz and Szlenk, 1980], the topological entropy is defined as

$$h(f) = \lim_{n\to\infty} \frac{1}{n} log(c_n),$$

$$h(f) \leq \frac{1}{n} log(c_n) : \text{ for any } n.$$

Topological entropy can be positive or zero and it is invariant under topological conjugacy. A dynamical system is said to be 'simple' if its topological entropy is equal to zero. Topological entropy is a measure of chaotic behaviour and chaos can be recognized with positive topological entropy.

Let f be a continuous interval map on I to itself. A set $U \in I$ is said to be scrambled set if there exists $\delta > 0$ such that every $x, y \in U$ with $x \neq y$, satisfies the following conditions:

$$\liminf_{n\to\infty} | f^n(x) - f^n(y) | = 0 \text{ and } \limsup_{n\to\infty} | f^n(x) - f^n(y) | \geq \delta.$$

By Li and Yorke [Li and Yorke, 1975], f is called chaotic if there is an uncountable scrambled set $U \subset I$.

Relationship between topological entropy and Li-Yorke chaos for the continuous interval map proved in [Blanchard *et al.*, 2002]. According to which positive topological entropy is sufficient condition for the map to be chaotic in the sense of Li and Yorke. Converse of the statement is not true in general.

If f and g are two unimodal maps and $K(f) \preceq K(g)$ then By [Block *et al.*, 1989], we have $h(f) \leq h(g)$. Here, $K(f)$ denotes the kneading sequence of f.

Algorithm for computing topological entropy

We discuss the following algorithm for computing topological entropy of the map $\mathscr{G}_{a,q_1}(x)$. We compare the kneading sequence $K(\mathscr{G})$ with the kneading sequence of tent map $K(T_s)$ with slope $s \in [1,2]$ whose entropy is known. The algorithm is given in the following steps:

(1) Choose the accuracy ε for the entropy and take a positive integer N (length of kneading sequence) such that $\frac{1}{N} < \varepsilon$.

(2) For fixed parameter a and q_1, iterate the map $\mathscr{G}_{a,q_1}(x)$ taking critical point as initial point with N times and find the kneading sequence $K(\mathscr{G})$.

(3) Take $a_1 = 1$ and $b_1 = 2$, the initial bound of the slope $s \in [a_1, b_1]$.

(4) Take slope $s = \frac{a_1+b_1}{2}$.

(5) Compute $K(T_s)$ with the slope s i.e. $\frac{a_1+b_1}{2}$.

(6) Compare $K(\mathscr{G})$ with $K(T_s)$:

- If $K(\mathscr{G}) \geq K(T_s)$ then $h(\mathscr{G}) \geq K(T_s)$ so define $a_1 = s$ and the next interval bound for the slope is $[s, b_1]$.
- If $K(\mathscr{G}) \leq K(T_s)$ then $h(\mathscr{G}) \leq K(T_s)$ so define $b_1 = s$ and the next interval bound for the slope is $[a_1, s]$.

(7) If $b_1 - a_1 < \varepsilon$ then $h(\mathscr{G}) = \log(\frac{a_1+b_1}{2})$ otherwise go to step-4.

(8) Repeat the step 2 to step 7 for the different value of parameter a and q_1.

We have implemented the above algorithm using the software MATLAB for the map $\mathscr{G}_{a,q_1}(x)$ by taking $\varepsilon = 0.001$ and $N = 1001$. For $a \in (3.5, 4)$ and $q_1 \in (0, 1)$, the graph of topological entropy is shown in Fig. 2.4 and the level curves are shown in Fig. 2.5.

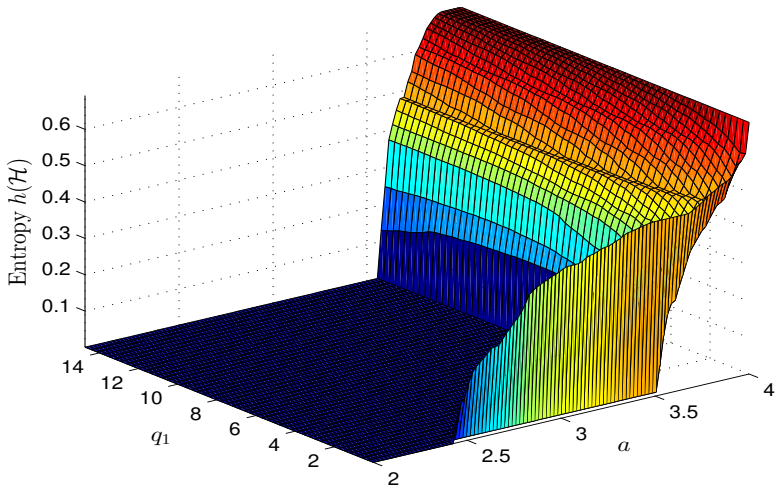

Figure 2.4. : Topological entropy of the map $\mathscr{G}_{a,q_1}(x)$ for $a \in (2,4)$ and $q_1 \in (0,15)$.

In the Fig. 2.5, dark blue colour shows the map with zero topological entropy and all other colours are corresponding to the maps of positive topological entropy. The value of the entropy changes when the bifurcation occur. The zoom part of level curve for values $q_1 \in (0, 0.05)$ are shown in Fig. 2.5(ii). The minimum of a_∞ (where transition takes place from simple to chaotic dynamics) among $q_1 \in (0, 15)$ can be observe nearly at $a = 2.5$. For different q_1, the values of a_∞ are given in Table 2.1. At $q_1 = 0.02$, the map $\mathscr{G}_{a,q_1}(x)$ has $a_\infty = 3.248973$ which is very much less than the $a_\infty = 3.56995\ldots$ of usual logistic map (2.1). This illustrate the fact that the phase transition of q-deformed map occurs much earlier than the canonical logistic map.

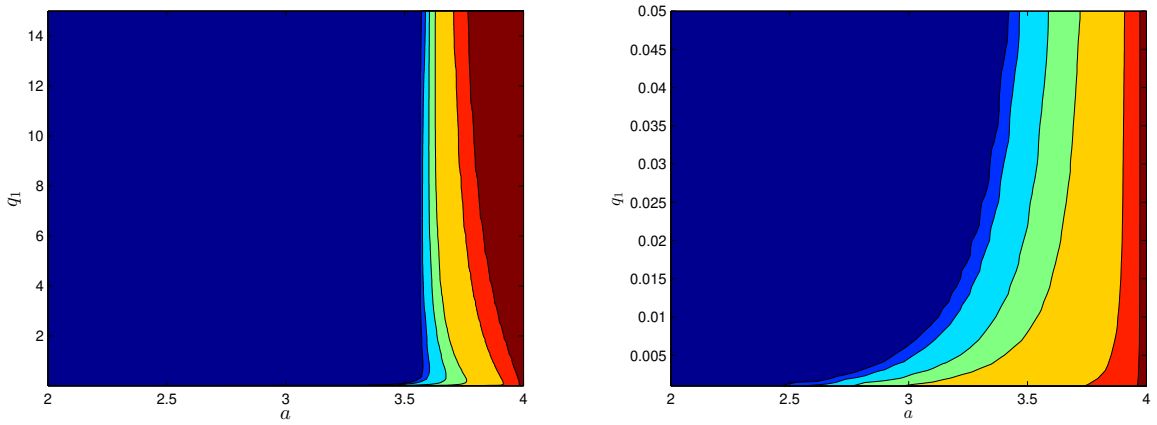

(i) (ii)

Figure 2.5. : Level curves of the map $\mathscr{G}_{a,q_1}(x)$ for $a \in (2,4)$; (i) $q_1 \in (0,15)$; (ii) $q_1 \in (0.001, 0.05)$.

q_1	a_∞
10^{-3}	2.435607
0.02	3.248973
0.1	3.478148
0.5	3.565168
0.8	3.57004
0.9	3.57015
0.999	3.560947

Table 2.1. : The value of parameter a where topological entropy turns zero to positive for $q_1 \in (0,1)$.

2.3 Q-LOGISTIC MAP OF TYPE-2

Type-2 deformation on the real number x and deformed parameter q_2 is given by

$$[x]_{q_2} = \frac{{q_2}^x - {q_2}^{-x}}{q_2 - {q_2}^{-1}}, \tag{2.5}$$

where $q_2 \in (0,\infty) \setminus \{1\}$ with the required property that $q_2 \to 1$ then the deformed number $[x]_{q_2} \to x$.

We apply deformation $[x]_{q_2}$ on x of $f_a(x)$ given in Eq. (2.1) then we obtain the q-logistic map of type-2 as

$$\mathsf{H}_{a,q_2}(x) = [\cdot]_{q_2} \circ f_a(x),$$

which implies

$$\mathsf{H}_{a,q_2}(x) = \frac{q_2^{ax(1-x)} - q_2^{ax(x-1)}}{q_2 - q_2^{-1}}, \tag{2.6}$$

where $a \in [0,4]$ and $x \in [0,1]$. For the investigation of properties of $\mathsf{H}_{a,q_2}(x)$, we choose the bounded domain $q_2 \in (1,30)$. The map $\mathsf{H}_{a,q_2}(x)$ is an interval map from [0,1] to [0,1] and it has unique critical point at $x = 0.5$.

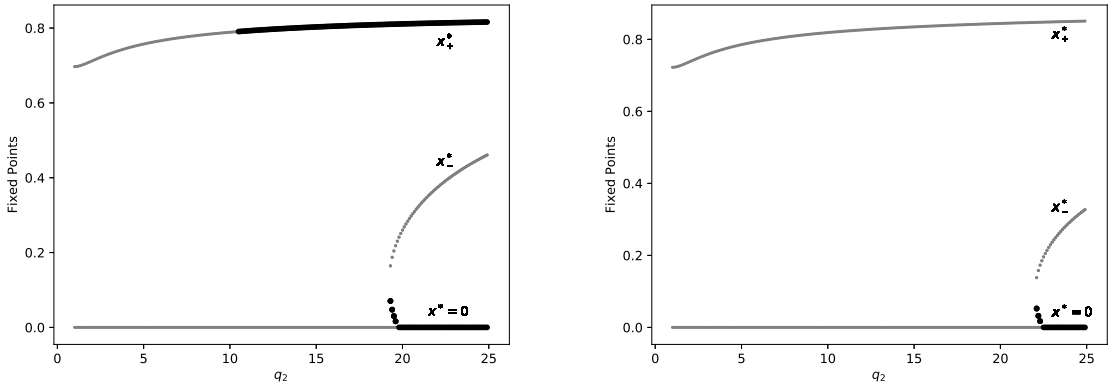

(i) $a = 3.3$ (ii) $a = 3.6$

Figure 2.6. : Fixed points of the map $\mathsf{H}_{a,q_2}(x)$ for deformed parameter $q_2 \in (1.001, 25)$.

The fixed points of type-2 q-logistic map $\mathsf{H}_{a,q_2}(x)$ cannot be solve analytically. Since the map $\mathsf{H}_{a,q_2}(x)$ is a transcendental equation, therefore we compute fixed points numerically. The fixed points of $\mathsf{H}_{a,q_2}(x)$ are shown in Fig. 2.6(i) and Fig. 2.6(ii) for $a = 3.3$ ans $a = 3.6$ respectively. The black line represents the stable fixed point and grey line represents the unstable fixed point. The zoom parts of the Fig. 2.6 around the bifurcation threshold is shown in Appendix Fig. B.1. From the Figs. 2.6(i) and 2.6(ii), we observe that as the deformed parameter q_2 varies from 30 to 1, initially there are three fixed points, namely x^*, x_+^* and x_-^*, and later x_-^* will disappear. The fixed point x_+^* undergoes reverse period doubling bifurcation route to chaos. The fixed point $x^* = 0$ exists as coexistence of attractor with other attractors. In fact, whenever there is coexistence of attractors then x_-^* is a repelling fixed point between these attractors. As the fixed point $x^* = 0$ become unstable, the repelling fixed point x_-^* also vanishes and the map has unique attractor.

The size of basin of the fixed point x^* is denoted by $\omega_1(x^*)$. We plot the basin of attraction of the fixed point $x^* = 0$ to obtain the region of coexistence of attractor, which is depicted in the Fig. 2.7(i). The region $R_1 \cup R_2$ where all initial conditions attracted towards x^* i.e. $\omega_1(x^*) = 1$ is indicated by blue region. The region R_3 where all initial conditions are attracted towards unique attractor except x^* i.e. $\omega_1(x^*) = 0$, which is shown as red region. The region R_4 where two or more attractor coexists i.e. $0 < \omega_1(x^*) < 1$ is shown by the green region. We are also interested in the region where $x^* = 0$ coexists with chaotic attractor. We calculate Lyapunov exponent to highlight the chaotic region. In the Fig. 2.7(ii), the region R_4 of coexisting attractor is shown as green colour, and chaotic region with positive Lyapunov exponent is shown as black colour. We consider the initial condition $x_0 = 0.5$ for computing the Lyapunov exponent. The coexistence of attractors can be visualized by the bifurcation diagram shown in Appendix Fig. B.2. The fixed point $x^* = 0$ shown in blue colour, coexists with chaotic attractor shown in black colour.

Proposition 2.3.1. *There is an open interval $(\gamma_1, \gamma_2) \subset [0,4]$ for every $(q_2, a) \in R_2$ such that there exists some states $x_i, x_j \in [0,1]$ for which there exists $n_0 \in \mathbb{N}$ such that*

$$\mathsf{H}^n_{a,q_2}(x_i) \to x_-^* \text{ and } \mathsf{H}^n_{a,q_2}(x_j) \to 0 \text{ for all } n \geq n_0.$$

Proof is similar to the Proposition 2.2.2.

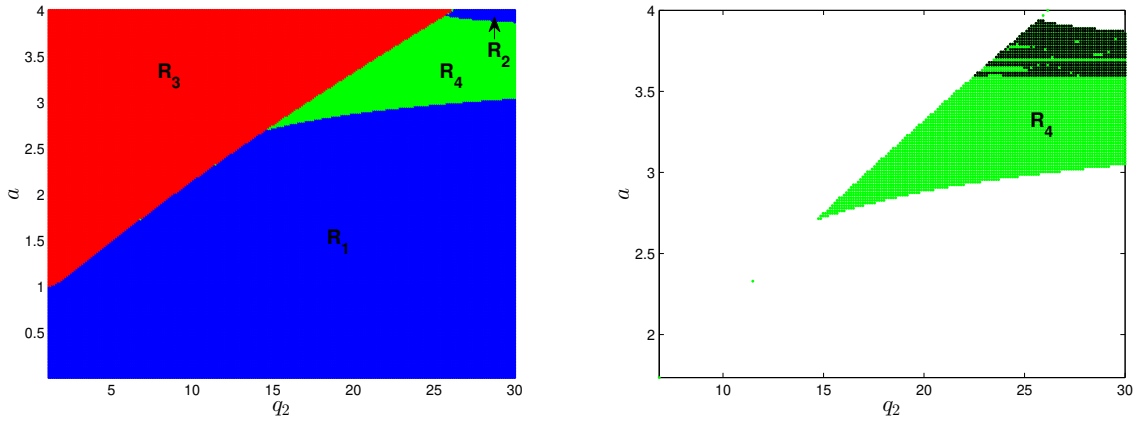

(i) (ii)

Figure 2.7. : (i) Basin of attraction of the fixed point $x^* = 0$; (ii) Coexistence of attractors with chaotic attractor (black colour).

We calculate the topological entropy of the map $\mathsf{H}_{a,q_2}(x)$ with the algorithm given in Section 2.2.2 using the software MATLAB. The topological entropy of the map $\mathsf{H}_{a,q_2}(x)$ is shown in Fig. 2.8(i), and the level curve is shown in Fig. 2.8(ii) for $a \in (3.5,4)$ and $q_2 = (1,30)$. The map with zero topological entropy is shown in dark blue colour on the level curve Fig. 2.8(ii), whereas the rest of colours represents maps with positive topological entropy. We get higher entropy maps as the parameter a increases. We observe that as q_2 approaches to 1, we obtain positive topological entropy with smaller value of the parameter a. The minimum of a_∞, where transition takes place from simple to chaotic region obtained nearly at $q_2 = 1.0001$, $a_\infty = 3.56995\ldots$. It is clear from Fig. 2.8(ii) that for $q_2 \neq 1$, the a_∞ of the map $\mathsf{H}_{a,q_1}(x)$ is greater than the $a_\infty = 3.56995\ldots$ of the canonical logistic map.

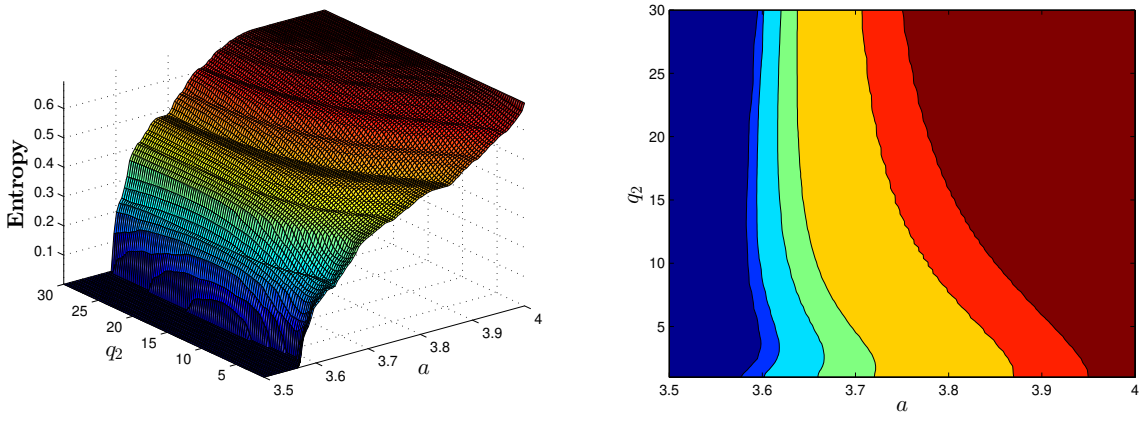

(i) (ii)

Figure 2.8. : (i) Topological entropy of the map $\mathsf{H}_{a,q_2}(x)$ for $a \in (3.5,4)$ and $q_2 \in (1,30)$; (ii) Level curve.

2.4 Q-GAUSSIAN MAP OF TYPE-1

Let $g_c(x)$ be the Gaussian map, which is given by

$$g_c(x) = e^{-bx^2} + c, \tag{2.7}$$

where $b \neq 0$ and c is real parameter. This one-dimensional interval map with two-parameters qualitatively describes the dynamics of electrical circuit with a nonlinear diode which shows chaotic behaviour.

Applying type-1 deformation given by Eq. (2.2) on x of $g_c(x)$ then we obtain the following q-deformed Gaussian map.

$$\begin{aligned} g_c([x]_{q_1}) &= e^{-b\left(\frac{1-q_1^x}{1-q_1}\right)^2} + c, \\ &\equiv G_{c,q_1}(x). \end{aligned} \tag{2.8}$$

We call it as q-Gaussian map of type-1. This is an one-dimensional unimodal map with three parameters b, c and deformed parameter q_1, where $q_1 > 0$, $b > 0$ and $c \in (-1,1)$. In this discussion we consider $b = 7.5$, $q_1 \in (0,2) \setminus \{1\}$ and $c \in (-1,1)$. As $q_1 \to 1$, the deformation $[x]_{q_1} \to x$, the original Gaussian map can be obtained.

Remark 2.4.1. *The map* $G_{c,q_1}(x) = e^{-b\left(\frac{1-q_1^x}{1-q_1}\right)^2} + c$, *satisfies the following properties:*

1. *The unique critical point of* $G_{c,q_1}(x)$ *is* $C = 0$ *which is non-degenerate i.e.,* $G''_{c,q_1}(0) \neq 0$.
2. *The maximum value is attained at* $x = 0$ *which is* $1 + c$.
3. $G_{c,q_1}(x)$ *is of class* C^∞ *and has negative Schwarzian derivative,*

$$S(g \circ [\cdot]_{q_1}) = (S(g) \circ [\cdot]_{q_1}) \cdot ([x]'_{q_1})^2 + S([\cdot]_{q_1})(x),$$

where $S(g)(x) = \frac{-4b^2x^4+3}{2x^2}$ *and* $S([\cdot]_{q_1})(x) = \frac{-(\log q_1)^2}{2}$.

Since,

$$\begin{aligned} S(G_{c,q_1})(x) &= S(g \circ [\cdot]_{q_1})(x), \\ &= -\frac{1}{2}(\log q_1)^2 \left(\frac{4b^2(q_1^x)^2\{(1-q_1^x)^4 + 3(1-q_1)^4\}}{2(1-q_1^x)^2(1-q_1)^4} + 1 \right). \end{aligned}$$

Hence $S(G_{c,q_1})$ *is negative for all* c *and* q_1.

2.4.1 Fixed points and periodic attractors

The q-Gaussian map $G_{c,q_1}(x)$ is a transcendental equation so we need to employ Newton-Raphson method to get the fixed points of the map. As the parameter c varies from -1 to 1, initially we get three fixed points in an order $x^* < x^*_- < x^*_+$. Out of these three fixed points, two of them x^* and x^*_- are negative and other one x^*_+ is positive. Later we have only one fixed point x^*_+. For the different values of q, fixed points of the map are shown in Fig. 2.9. The thick line (black colour) indicates the stable fixed points whereas the thin line (grey colour) indicates unstable fixed

points. The fixed point x^* exists as co-existing attractor with other periodic attractors. Whenever, there is bistability of attractor, the x^*_- exits as unstable fixed point between these attractors. In the region where x^*_+ is unstable we have other metric attractors (periodic orbit, a Cantor set or a transitive interval attractor). The q-Gaussian map undergoes period doubling route to chaos. The superstable periodic orbits of period-2^n of $G_{c,q_1}(x)$ are given in Appendix Table B.1.

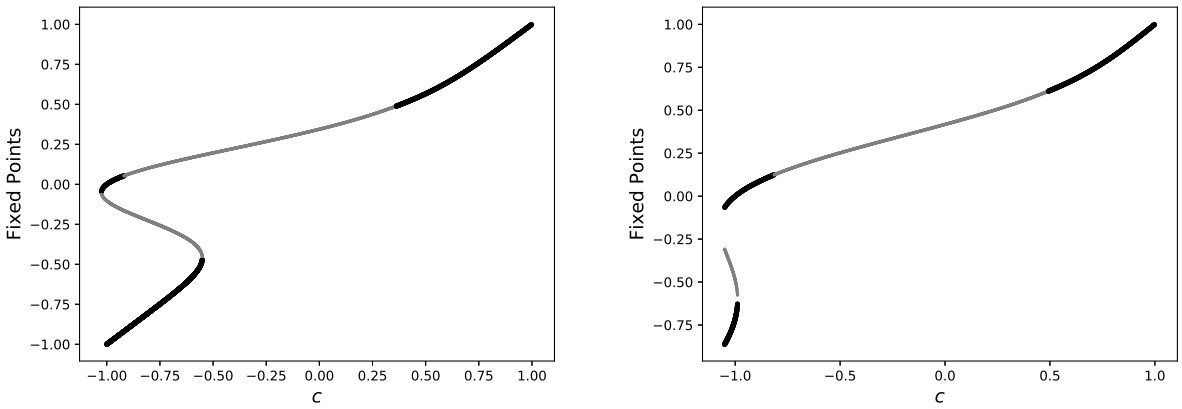

(i) $q_1 = 0.75$ (ii) $q_1 = 1.9$

Figure 2.9. : Fixed points of q-Gaussian map of type-1 $G_{c,q_1}(x)$ for $c \in (-1,1)$.

2.4.2 Topological entropy by lap number method

Let us consider class $\mathscr{F}$ of C^2 maps $f : [a_1,b_1] \to [a_1,b_1]$ with a critical point at $x_c \in (a_1,b_1)$, and satisfy the following;

(I) $f''(x_c) < 0$

(II) $f'(x) > 0$ for $x < x_c$ and $f'(x) < 0$ for $x > x_c$.

Topological entropy of $f \in \mathscr{F}$ can be calculated through the minimal number of monotonic pieces or laps of the iterates f^n. Let l_n be the minimal number of monotonic pieces of f^n, then the topological entropy of f is given by

$$h_1(f) = \lim_{n\to\infty} \sup \frac{1}{n} log(l_n). \tag{2.9}$$

To calculate the lap number l_n of the function $f \in \mathscr{F}$, we use the following Theorem by R. Dilao [Dilao and Amigó, 2012].

Theorem 2.4.2. *Let $\Omega = (\Omega_k)_{k\geq 1}$ be a sequence of $f \in \mathscr{F}$, and set,*

$$J_n = \{1 \leq j \leq n : \Omega_j \in \mathscr{M}\},$$

where $\mathscr{M} = \{m^+, M^-, m^0, M^0\}$. Let $(\alpha_k)_{k\geq 1}$ and $(\beta_k)_{k\geq 1}$ be the sequences defined below, then

$$l_{n+1} = 2l_n - 2\sum_{j\in J_n} (l_{n+1-j} - l_{n-j}) - \alpha_n - \beta_n, \tag{2.10}$$

where $l_0 = 1$ and $n \geq 1$.

The procedure is to calculate the topological entropy is as follows:

(1) Let $\Theta_f(x)$ be a sequence with entries $\Theta f,n(x)$ where $n \geq 0$.

$$\Theta_{f,n}(x) = \begin{cases} 1 & \text{if } f^n(x) > x_c, \\ 0 & \text{if } f^n(x) = x_c, \\ -1 & \text{if } f^n(x) < x_c. \end{cases}$$

(2) Define another sequence Ω_f with entries $\Omega_{f,n}$ where $n \geq 1$. Entries of Ω_f belonging to the alphabets $\{M^+, M^-, M^0, m^+, m^-, m^0\}$. The sign of $\Theta f,n(x_c)$ decides the sign of symbols of $\Omega_{f,n}$. The symbol can be decide as if $\prod_{i=0}^{i=n-1} \Theta_{f,i}(x_c)$ is odd then symbol m otherwise M.

(3) The functions $\lambda(k)$ and $\rho(k)$ with $\lambda(0) = \rho(0) = 0$ and for $k \geq 1$

$$\lambda(k) = \begin{cases} 0 & \text{if } \operatorname{sign}(f^k(a_1) - x_c) \cdot \operatorname{sign}(f^{1+\lambda(k-1)} - x_c) < 0, \\ 1 & \text{if } \operatorname{sign}(f^k(a_1) - x_c) \cdot \operatorname{sign}(f^{1+\lambda(k-1)} - x_c) \geq 0. \end{cases}$$

$$\rho(k) = \begin{cases} 0 & \text{if } \operatorname{sign}(f^k(b_1) - x_c) \cdot \operatorname{sign}(f^{1+\lambda(k-1)} - x_c) < 0, \\ 1 & \text{if } \operatorname{sign}(f^k(b_1) - x_c) \cdot \operatorname{sign}(f^{1+\lambda(k-1)} - x_c) \geq 0. \end{cases}$$

(4) The sequence α_k and β_k can be calculated as

$$\alpha_k = \begin{cases} 0 & \text{if } \lambda(k) = 0, \\ 0 & \text{if } \lambda(k) \neq 0 \text{ and } \Omega_{1+\lambda(k-1)} \in \mathscr{M}, \\ 1 & \text{if } \lambda(k) \neq 0 \text{ and } \Omega_{1+\lambda(k-1)} \notin \mathscr{M}. \end{cases}$$

$$\beta_k = \begin{cases} 0 & \text{if } \rho(k) = 0, \\ 0 & \text{if } \rho(k) \neq 0 \text{ and } \Omega_{1+\rho(k-1)} \in \mathscr{M}, \\ 1 & \text{if } \rho(k) \neq 0 \text{ and } \Omega_{1+\rho(k-1)} \notin \mathscr{M}, \end{cases}$$

where $\mathscr{M} = \{m^+, M^-, m^0, M^0\}$.

(5) Lap number l_n can be calculated using Theorem 2.4.2.

(6) Put the value of l_n in Eq. (2.9) to evaluate topological entropy $h_1(f)$.

We implement the above algorithm using the software MATLAB to calculate the topological entropy of the map $G_{c,q_1}(x)$, which is depicted in Figs. 2.10 and 2.11.

The topological entropy and Lyapunov exponent of q-Gaussian map $G_{c,q_1}(x)$ are shown in Fig. 2.10 for fixed q_1. The region where topological entropy is positive taken as chaotic region. As q_1 increases from 0 to 2, the chaotic region of $G_{c,q_1}(x)$ gets contracted and after particular value of q_1 there is no chaotic region, which is illustrated in Fig. 2.10. The topological entropy for $c \in (-1,0)$ and $q_1 \in (0,2)$ is shown in Fig. 2.11(i) and its level curve is shown in Fig. 2.11(ii). The dark blue colour indicates the map with zero topological entropy and rest of the colours is for positive topological entropy. We observe that as the deformation parameter $q_1 \to 0$, the map $G_{c,q_1}(x)$ has positive topological entropy for wide range of parameter c.

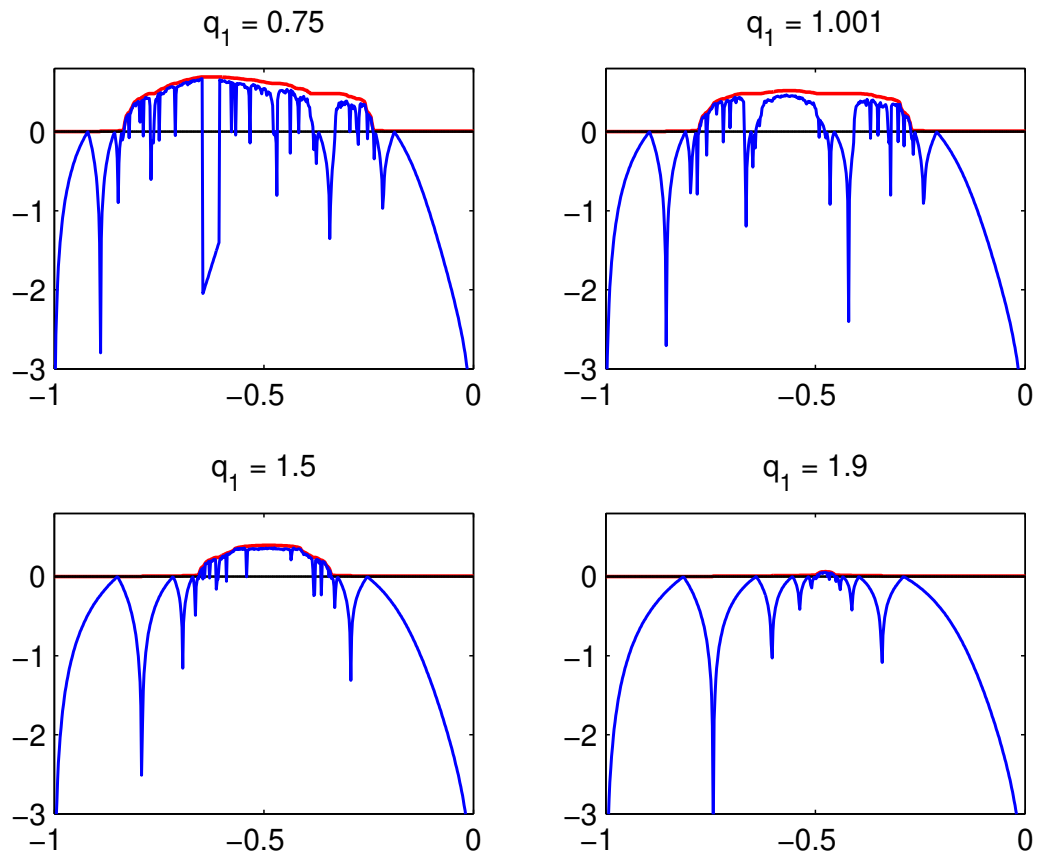

Figure 2.10. : Topological entropy and Lyapunov exponent of the map $G_{c,q_1}(x)$ are shown in red and blue colours respectively at $b = 7.5$, and x axis denotes $c \in (-1, 0)$. We consider the initial condition $x_0 = -0.1$ for computing the Lyapunov exponent.

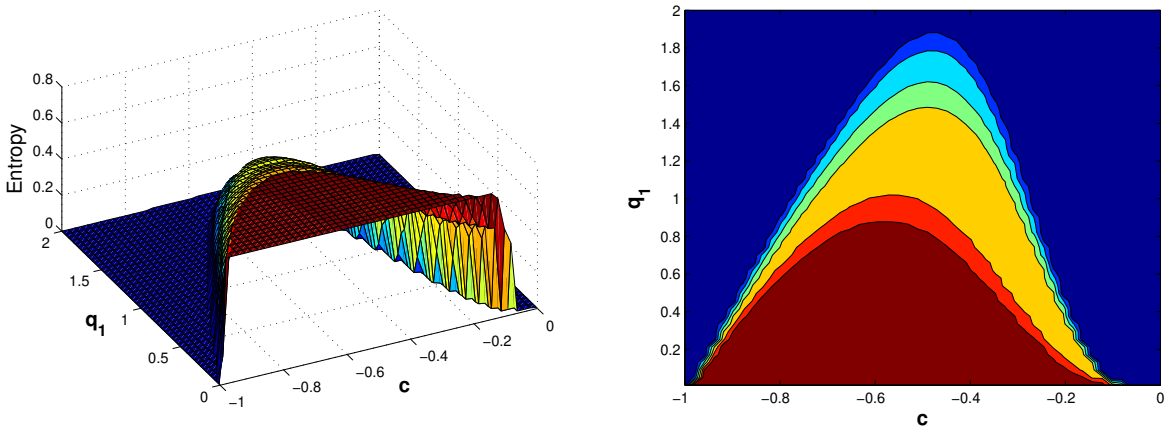

(i) (ii)

Figure 2.11. : (i) Topological entropy of the map $G_{c,q_1}(x)$ as c and q_1 varies; (ii) Level curve.

2.5 CONCLUSIONS

In this chapter, we have applied type-1 deformation scheme on the logistic map (Eq.(2.2)) and analyzed the basic dynamics and dynamic paradox. We observed that the transition from simple to chaotic dynamics of q-logistic map of type-1 happened much earlier than the canonical logistic map. The composition of two simple maps, deformation map $[x]_{q_1}$ and logistic map $f_a(x)$ (for $a < a_\infty$) turns to be chaotic, which shows the Parrando's paradox in q-logistic map of type-1.

We have computed the topological entropy to prove the existence of Li-Yorke chaotic maps and highlights the region where the chaos found to be unobservable. The topological entropy of the map $\mathscr{G}a, q_1(x)$ (Eq.(2.4)) is positive in this region whereas all the trajectories seems to converge at $x^* = 0$. But this will not happen. Further, we notice that there is a set of totally disconnected points which do not converge to $x^* = 0$.

We also calculated the topological entropy of the q-logistic map of type-2 and observed that the a_∞ value (where the transition takes place from simple to chaotic behavior) of q-logistic of type-2 is larger than a_∞ value of canonical logistic map. Therefore, we conclude that there is a delay in the phase transition for this deformed map. This is contrary to the type-1 q-logistic map, where the phase transition happens earlier than the canonical logistic map.

In the type-1 deformed Gaussian map (Eq.(2.8)) we have analyzed the basic dynamics and computed the topological entropy by using Lap number method. From this analysis we conclude that there exist Li-Yorke chaos and also the region of unobservable chaos.